Dalton Transactions

PAPER

View Article Online
View Journal

Cite this: DOI: 10.1039/c6dt01077f

Synergistic oxygen atom transfer by ruthenium complexes with non-redox metal ions†

Zhanao Lv, Wenrui Zheng, Zhuqi Chen,* Zhiming Tang, Wanling Mo and Guochuan Yin*

Received 19th March 2016,
Accepted 7th June 2016

DOI: 10.1039/c6dt01077f

www.rsc.org/dalton

Non-redox metal ions can affect the reactivity of active redox metal ions in versatile biological and heterogeneous oxidation processes; however, the intrinsic roles of these non-redox ions still remain elusive. This work demonstrates the first example of the use of non-redox metal ions as Lewis acids to sharply improve the catalytic oxygen atom transfer efficiency of a ruthenium complex bearing the classic 2,2′-bipyridine ligand. In the absence of Lewis acid, the oxidation of ruthenium(II) complex by $PhI(OAc)_2$ generates the Ru(IV)═O species, which is very sluggish for olefin epoxidation. When $Ru(bpy)_2Cl_2$ was tested as a catalyst alone, only 21.2% of cyclooctene was converted, and the yield of 1,2-epoxycyclooctane was only 6.7%. As evidenced by electronic absorption spectra and EPR studies, both the oxidation of Ru(II) by $PhI(OAc)_2$ and the reduction of Ru(IV)═O by olefin are kinetically slow. However, adding non-redox metal ions such as Al(III) can sharply improve the oxygen transfer efficiency of the catalyst to 100% conversion with 89.9% yield of epoxide under identical conditions. Through various spectroscopic characterizations, an adduct of Ru(IV)═O with Al(III), Ru(IV)═O/Al(III), was proposed to serve as the active species for epoxidation, which in turn generated a Ru(III)–O–Ru(III) dimer as the reduced form. In particular, both the oxygen transfer from Ru(IV)═O/Al(III) to olefin and the oxidation of Ru(III)–O–Ru(III) back to the active Ru(IV)═O/Al(III) species in the catalytic cycle can be remarkably accelerated by adding a non-redox metal, such as Al(III). These results have important implications for the role played by non-redox metal ions in catalytic oxidation at redox metal centers as well as for the understanding of the redox mechanism of ruthenium catalysts in the oxygen atom transfer reaction.

Introduction

Ruthenium based compounds have attracted continuous attention because they are versatile synthetic tools for selective oxidation processes in both homogeneous and heterogeneous conversions, including asymmetric epoxidation of olefins,[1–11] oxidation of alcohols,[12–16] oxidative esterification,[17–19] C–C coupling,[20–23] oxidation of aryl sulfides,[24–26] and water oxidation.[27–32] In most cases, the active site of the Ru center is recognized as a Ru═O group in which ruthenium is in a formal high oxidation state (Ru(IV) or Ru(VI)).[3,5,33–40] Due to the rich oxidative properties of the Ru═O species, a large number of examples related to ruthenium catalysts have emerged recently, and the oxidation mechanisms of Ru═O species have been thoroughly investigated. Attempts have been made to optimize the performance of ruthenium catalysts through chemical modification of their attached organic ligands.[6,18,29,41–44] However, chemical modification of organic ligands still has major drawbacks, such as high cost, unpredictable stability, and time-consuming procedures; examples also exist where unexpected steric hindrance in the first coordination sphere strongly influences the reactivity of a Ru═O system.[24,43]

Alternatively, non-redox metal ions serving as Lewis acids offer another efficient strategy for regulating the reactivity of redox metal ions through bridging or ligation with the metal-oxo or metal-hydroxo moiety in a variety of homogeneous chemical transformations. The role of these non-redox metal ions has attracted much attention in both the biological and chemical communities because understanding how these non-redox metal ions participate in oxidation events and affect the reactivity of redox-active metal ions is highly important for understanding the mechanism of metalloenzymes,[45–48] such as the essential roles of Ca(II) in Photosystem II in water oxidation.[49] On the other hand, many non-redox metal ions are

Key laboratory of Material Chemistry for Energy Conversion and Storage (Huazhong University of Science and Technology), Ministry of Education, Key laboratory of Material Chemistry and Service Failure, School of Chemistry and Chemical Engineering, Huazhong University of Science and Technology, Wuhan 430074, PR China. E-mail: zqchen@hust.edu.cn, gyin@hust.edu.cn

† Electronic supplementary information (ESI) available: Crystallographic data in CIF and GC-MS graph, NMR and HSQC spectra, UV-Vis absorption spectra or other reaction information. CCDC 1411258. For ESI and crystallographic data in CIF or other electronic format see DOI: 10.1039/c6dt01077f

frequently employed as additives to improve the stability and/or to manipulate the activity of transition metal catalysts; however, their pivotal role is still elusive.[50,51]

To date, the available examples of adding Lewis acids to manipulate the stoichiometric oxidation properties of transition metals include manganese,[52–56] iron,[57–61] cobalt[62,63] and osmium[64] complexes. Collins found that non-redox metal ions can accelerate triphenylphosphine oxygenation by their (TAML)Mn(v)(O) analogues but do not improve olefin epoxidation.[52] Borovik showed that Ca(II) has a marked influence on the rate of dioxygen activation by a monomeric Mn(II) complex, and a heterobimetallic complex containing Mn(III)–(μ-OH)–Ca(II) cores was confirmed by its single crystal X-ray structure.[56] Goldberg observed that Zn(II) may interact with the Mn(V)≡O group in a (corrolazine)Mn(V)(O) complex and accelerate its rate in both hydrogen abstraction and electron transfer reactions.[55,65,66] Nam and Fukuzumi revealed that binding Sc(III) to (N4Py)Fe(IV)(O) complex can accelerate electron-transfer reactivity because of a large positive shift in the one-electron reduction potential by binding the Sc(III) cation.[59] Also, the mechanism of sulfoxidation by Fe(IV)═O was changed from a direct oxygen atom transfer pathway to an electron transfer pathway.[58] Lau also demonstrated that adding $FeCl_3$ as a Lewis acid can accelerate catalytic alkane oxidation by generating a $[Os(VIII)(N)(O)Cl_4]^-$/Lewis acid adduct.[64] Borovik further accomplished the synthesis and characterization of a Co(III)–(μ-OH)–Ca(II) complex and revealed the changes in the redox properties of Co(II) complexes correlated with the coordination of Ca(II).[63]

The above findings clearly demonstrate that non-redox metal ions as Lewis acids can modulate the redox behaviors of high valent transition metal ions, although in most examples, only accelerated electron transfer rates were observed. In particular, most of these reported examples are based on stoichiometric oxidations, while the examples of Lewis-acid-accelerated catalytic oxidation, which are more analogous to biological metalloenzymes and chemical oxidations by redox oxide catalysts, remain limited. Recently, we found that the presence of non-redox metal ions such as Al(III) can accelerate the catalysis of sulfide oxidation by a manganese complex having a cross-bridged cyclam ligand.[53] Moreover, we observed the first example in which non-redox metal ions greatly promote the catalytic epoxidation of olefin by dissociating the sluggish Mn(III)–$(\mu\text{-O})_2$–Mn(IV) species and generating the M^{n+}═O/Lewis acid adduct as the active species.[54] Inspired by the above findings, we wished to discern whether the addition of non-redox metal ions could also manipulate the physical and chemical properties of a Ru catalyst by interacting with the Ru═O species. In contrast to the extensive studies on optimizing the performance of the ruthenium catalyst through chemical modification of its organic ligands, introducing non-redox metal ions as additives demands no extra synthetic procedures and can be easily performed. More importantly, understanding how the electronic and catalytic properties of these complexes in various states are modulated by non-redox metal ions will provide more information on the mechanistic aspects of the oxidation, which can also be useful in heterogeneous catalysis as well as biological metalloenzymes.

Ruthenium imine complexes, such as $[Ru(bpy)_n]^{2+}$ (bpy = 2,2′-bipyridine), are among the most well-known ruthenium complexes and have been investigated extensively as analogues to natural chromophores for utilization in water oxidation as well as key materials and building blocks for various photonic/electronic devices.[29,32,67–70] Thus, the fundamental knowledge of the redox properties of bpy based Ru═O species is of paramount importance to understand and optimize its redox performance. However, the examples of catalytic oxidation by $[Ru(bpy)_n]^{2+}$ are surprisingly limited; to the best of our knowledge, no example of an efficient oxygen atom transfer reaction catalyzed by $[Ru(bpy)_n]^{2+}$ has been reported. Here, we present a non-redox metal ion-promoted oxygen atom transfer reaction with ruthenium imine complexes for the first time. The addition of Al(III) dramatically accelerated the epoxidation of cyclooctene to a yield of 89.9% with the *cis*-$Ru(bpy)_2Cl_2$ catalyst, whereas a yield of only 6.7% can be achieved with the ruthenium(II) complex alone. A comprehensive mechanism explaining this Lewis acid-accelerated-epoxidation was further investigated and may shed some light on the factors that favor the oxidation reactivity of ruthenium catalysts; it also illustrates a novel strategy to improve the catalytic reactivity of a variety of redox metal complexes.

Experimental section

The ruthenium(II) complex *cis*-$Ru(bpy)_2Cl_2$ was synthesized according to the literature.[44,71] Iodosobenzene diacetate ($PhI(OAc)_2$), sodium trifluoromethanesulfonate (NaOTf), magnesium trifluoromethanesulfonate ($Mg(OTf)_2$), and scandium trifluoromethanesulfonate ($Sc(OTf)_3$) came from Aladdin. Other trifluoromethanesulfonates, including $Ca(OTf)_2$, $Al(OTf)_3$, $Y(OTf)_3$ and $Ba(OTf)_2$, were purchased from Shanghai DiBai Chemical Company. Olefins and epoxides were purchased from either Aldrich or Alfa Aesar. $H_2{}^{18}O$ (97% ^{18}O atom) came from Aladdin. In all cases, solvents were dehydrated *via* 4 Å MS (activated at 400 °C for 2 h in a muffle furnace) prior to use. Di-2-pyridyl ketone (dpk), 2,2′-bipyrimidine (bpm) and 2,2′-bipyridine (bpy) were purchased from Sinopharm Chemical Reagents. 2,3-Bis(2-pyridyl) pyrazine (bpp) was from Aldrich and 1,10-phenanthroline-5,6-dione (ptd) was synthesized following the procedure in our previous publication.[72] The structures of these ligands have been illustrated in Scheme 1.

^{1}H NMR data of ligands: bpy (DMSO-d6): δ 7.47 (t, 2H), 7.96 (t, 2H), 8.40 (d, 2H), 8.70 (d, 2H); ptd ($CDCl_3$): δ 7.56 (m, 2H), 8.41 (m, 2H), 9.06 (m, 2H); bpm ($CDCl_3$): δ 7.38 (t, 2H), 8.95 (d, 4H); dpk ($CDCl_3$): δ 7.46 (m, 2H), 7.89 (m, 2H), 8.09 (m, 2H), 8.75 (m, 2H); bpp (DMSO-d6): δ 7.28 (m, 2H), 7.85 (m, 4H), 8.21 (m, 2H), 8.76 (m, 2H).

UV-Vis spectra were collected on an Analytik Jena Specord 205 spectrophotometer. GC-MS analysis was performed on an Agilent7890A/5975C system. EPR experiments were conducted

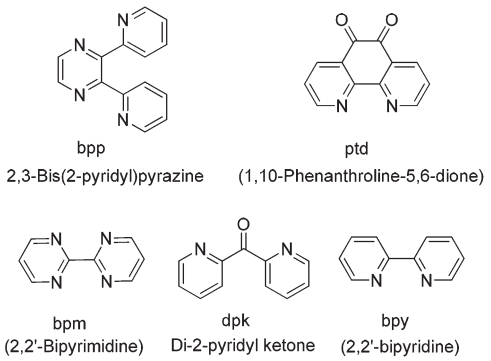

Scheme 1 Molecular structures of the ligands studied in this study.

at 130 K on a Bruker A200 instrument, with a center field of 3352.488 G, frequency of 9.395 GHz, power of 19.44 mW, modulation amplitude of 2.00 G and receiver gain of 1.00×10^3. X-Ray photoelectron emission spectra were obtained on a Kratos AXIS ULTRA DLD-600 W system, and all photoelectron peaks were referenced to the carbon C 1s peak at 284.4 eV. ^{1}H and ^{13}C NMR spectra were recorded on a Bruker AV-400 instrument using TMS as an internal reference; extra PhI and oxidant were removed by washing with cyclohexane.

General procedure for Lewis acid promoted catalytic epoxidation by ruthenium(II) complexes

A mixture solution of 0.8 mL of acetone and 0.2 mL of CH_2Cl_2 containing 1 mM ruthenium(II) complex, 2 mM 2,2′-bipyridine and 5 mM $PhI(OAc)_2$ was stirred at room temperature for 5 h. Then, 0.1 mmol olefin, 0.002 mmol Lewis acid and 0.2 mmol $PhI(OAc)_2$ were added to this solution. The reaction solution was stirred in a water bath at 308 K for 10 h. The yield of epoxide and the conversion of olefin were quantitatively analyzed by GC using the internal standard method. Control experiments with the ruthenium(II) complex or Lewis acid alone as the catalyst were carried out in parallel. The reactions were performed at least in triplicate, and the average data are used in the discussion.

General procedure for Lewis acid promoted catalytic epoxidation of *cis*- and *trans*-stilbene by ruthenium(II) complexes

A mixture solution of 0.8 mL of acetone and 0.2 mL of CH_2Cl_2 containing 1 mM ruthenium(II) complex, 2 mM 2,2′-bipyridine and 5 mM $PhI(OAc)_2$ was stirred at room temperature for 5 h. Then, 0.1 mmol olefin, 0.002 mmol Lewis acid and 0.2 mmol $PhI(OAc)_2$ were added to this solution. The reaction solution was stirred in a water bath at 298 K for 12 h. The yield of epoxide and the conversion of olefin were quantitatively analyzed by HPLC using the internal standard method, and the yield of benzaldehyde was quantitatively analyzed by GC using the internal standard method. Control experiments with the ruthenium(II) complex or Lewis acid alone as catalyst were carried out in parallel. The reactions were performed at least in triplicate, and the average data are used in the discussion.

General procedure for Lewis acid promoted catalytic epoxidation by ruthenium(II) complex in the presence of water

A mixture solution of 0.8 mL of acetone and 0.2 mL of CH_2Cl_2 containing 1 mM *cis*-$Ru(bpy)_2Cl_2$, 2 mM 2,2′-bipyridine and 5 mM $PhI(OAc)_2$ was stirred at room temperature for 5 h. Then, 0.1 mmol olefin, 0.002 mmol Lewis acid, 0.2 mmol $PhI(OAc)_2$ and a certain amount of water were added to this solution. The reaction solution was stirred in a water bath at 308 K for 10 h. The yield of epoxide and the conversion of olefin were quantitatively analyzed by HPLC using the internal standard method, and the yield of benzaldehyde was quantitatively analyzed by GC using the internal standard method. Control experiments with the ruthenium(II) complex or Lewis acid alone as the catalyst were carried out in parallel. Reactions were performed at least in triplicate, and the average data are used in the discussion.

Lewis acid promoted catalytic epoxidation by ruthenium(II) complex in the presence of ^{18}O-water

The mixture solution of 0.8 mL of acetone and 0.2 mL of CH_2Cl_2 containing 1 mM *cis*-$Ru(bpy)_2Cl_2$, 2 mM 2,2′-bipyridine and 5 mM $PhI(OAc)_2$ was stirred at room temperature for 5 h. Then 0.1 mmol olefin, 0.002 mmol Lewis acid, 0.2 mmol $PhI(OAc)_2$ and 0.1 mL $H_2{}^{18}O$ (97% ^{18}O enrichment as received) were added to this solution. The reaction mixture was stirred in a water bath at 308 K for 10 h, and the product analysis was performed by GC-MS using the same procedure as that used in normal epoxidation. The ^{18}O enrichments are calculated based on the peak abundances of ^{16}O- and ^{18}O-epoxide in the GC-MS graphs.

Crystal structure analysis

cis-$Ru(bpy)_2Cl_2$ (19.4 mg, 40 μmol), $Sc(OTf)_3$ (39.3 mg, 80 μmol) and $PhI(OAc)_2$ (64.4 mg, 200 μmol) were dissolved in acetonitrile (20 mL) followed by stirring at r.t. in air for 1 h. The solution color changed rapidly from purple to yellow. Single crystals of $Ru^{III}(bpy)_2(CF_3SO_3)Cl_2{\cdot}CH_3CN$ suitable for X-ray crystallography were grown by slow vapor diffusion of diethyl ether into the above reaction mixture at 5 °C. A red prism-shaped crystal with dimensions of 0.25 × 0.17 × 0.14 mm was selected for X-ray structure analysis. Intensity data for this compound were collected on a Bruker D8 Quest diffractometer at 173(2) K using graphite-monochromated Mo Kα radiation (λ = 0.71073 Å) with a ω-scan method. The centrosymmetric monoclinic space group $P2_1/n$ was determined by systematic absences and statistical tests and verified by subsequent refinement. The structure was solved by direct methods and refined by full-matrix least-squares methods on F^2. One target molecule was co-crystallized with 1 equiv. of acetonitrile. The crystal data and structure refinement results of $Ru^{III}(C_{10}H_8N_2)_2(CF_3SO_3)Cl_2$ are given in Tables S5–S8,† and the structure of the six-coordinate complex is shown in Fig. S7.†

Results and discussion

Synergistic effect in epoxidation

Initial assays were performed with cyclooctene as a test substrate, using dehydrated acetone/CH_2Cl_2 (4 : 1, v/v) as the solvent and $PhI(OAc)_2$ as the oxidant. The results obtained are compiled in Table 1, together with $Al(OTf)_3$ as an additive, for the purpose of comparison. *cis*-$Ru(bpy)_2Cl_2$ was initially used as the catalyst; hereafter, it will be referred to as $Ru(bpy)_2Cl_2$.

As listed in Table 1, when $Ru(bpy)_2Cl_2$ was tested as the catalyst alone, only 21.2% of cyclooctene was converted and the yield of 1,2-epoxycyclooctane was only 6.7%, indicating that $Ru(bpy)_2Cl_2$ is very sluggish in catalyzing cyclooctene epoxidation. When 2 equiv. of $Al(OTf)_3$ were added to the reaction solution, 100% conversion with 89.9% yield of epoxide could be achieved under the identical conditions. In a control experiment, $Al(OTf)_3$ alone as the catalyst provided only 15.2% conversion and 3.7% yield, which was close to the blank test as listed in entry 1 (12.4% conversion and 1.4% yield). Apparently, Lewis acid alone has almost no catalytic activity for olefin epoxidation in our case. In complementary experiments, $Ru(OTf)_3$ was used as the precursor to synthesize the ruthenium(II) catalyst *in situ*; this demonstrated very sluggish activity, providing only 12.9% of conversion with a 10.1% yield of epoxide, revealing that the promotional effect cannot be attributed to the presence of OTf^- anion. Meanwhile, a mixture of $Al(OTf)_3$ and bpy ligand as catalyst also showed very sluggish activity, in which only 18.0% conversion and 7.0% yield were achieved; this excluded the possibility that the synergistic effect originates from the potentially generated complex of Al(III) with the ligand. Therefore, this great improvement in the catalytic activity of the $[Ru(bpy)_2]^{2+}$ complex by adding non-redox metal ions Al(III) strongly supports that the synergistic effect occurs between the ruthenium catalyst and the Lewis acid in epoxidation. The addition of extra ligand (2,2′-bpy) can slightly improve the yield of epoxide by preventing the existence of ligand-free ruthenium species, which can lead to ring opening of epoxides with Lewis acid (Table S3†).

Given that the Ru^{II} complex in this work is a potential photosensitizer, the epoxidation of 1,2-cyclooctene was investigated in the dark; the results have been provided in Table S10 in the ESI.† The synergetic effect between $Ru(bpy)_2Cl_2$ and Lewis acid ($Al(OTf)_3$) was still found to occur in the dark. For example, a conversion of 11.5% and a yield of 4.2% were achieved by adding $Al(OTf)_3$, while for $Ru(bpy)_2Cl_2$, the conversion was 19.6% and the yield was 7.6% for the epoxide (Table S10†). Without any irradiation, epoxidation with $Ru(bpy)_2Cl_2$ and $Al(OTf)_3$ under identical conditions still showed efficient activity, with 99.8% conversion of the substrate and 90.2% yield of the epoxide (see Table S10 in the ESI†). Thus, these data clearly exclude the influence of the Ru^{II} complex as a potential photosensitizer.

This synergistic effect has also been observed by adding other non-redox metal ions to the reaction mixture. The addition of either Sc(III) or Y(III) provided 100% conversion, and the yields of epoxide were 72.5% and 73.1%, respectively. Non-redox metal ions with a positive charge of 2+, such as Mg(II), Ca(II), Ba(II) and Zn(II), also showed similar promotional effects. For example, adding 2 equiv. of Mg(II) or Ca(II) resulted in 100% conversion with epoxide yields of 77.0% and 72.6%, respectively, whereas Mg(II) or Ca(II) alone provided only 19.3% or 11.0% conversion with 2.5% or 4.4% yield in control experiments, respectively. Meanwhile, adding 6 equiv. of NaOTf only provided 21.9% conversion with 5.0% yield of epoxide, which was identical to the results of the control experiments without any additives (21.2% conversion with 6.7% yield). Because the concentration of OTf^- under these conditions is identical to that of 2 equiv. of $Al(OTf)_3$, the above results reveal that the promotional effect cannot be attributed to the presence of OTf^- anion. It is worth noting that in the control experiments, all of these non-redox metal ions alone as catalysts demonstrate very poor catalytic activity for epoxidation (Table 2).

The catalytic kinetics further confirms the promotional effect of Lewis acid on Ru(II) complex-mediated epoxidation (Fig. 1). In the presence of Ru(II) catalyst or Lewis acid alone, the catalytic epoxidation of cyclooctene is apparently sluggish,

Table 1 Influence of $Al(OTf)_3$ concentration on the catalytic oxidation of cyclooctene

Entry	Catalyst (1 mM)	Lewis acid	Conv. (%)	Yield (%)
1	—	—	12.4	1.4
2	$Ru(bpy)_2Cl_2$	—	21.2	6.7
3	—	$Al(OTf)_3$ (2 mM)	15.2	3.7
4	$Ru(bpy)_2Cl_2$	$Al(OTf)_3$ (0.5 mM)	30.3	9.9
5	$Ru(bpy)_2Cl_2$	$Al(OTf)_3$ (1 mM)	61.5	34.7
6	$Ru(bpy)_2Cl_2$	$Al(OTf)_3$ (2 mM)	99.9	89.9
7	$Ru(bpy)_2Cl_2$	$Al(OTf)_3$ (4 mM)	99.3	70.4
8[a]	$Ru(bpy)_2(OTf)_3$	—	12.9	10.1
9	bpy	$Al(OTf)_3$ (2 mM)	18.0	7.0

Conditions: acetone/CH_2Cl_2 (4 : 1, v/v) 1 mL, cyclooctene 0.1 M, ruthenium(II) catalyst 1 mM, 2,2′-bipyridine 2 mM, $PhI(OAc)_2$ 0.2 M, 308 K, 10 h. [a] $Ru(bpy)_2(OTf)_3$ was *in situ* synthesized by $Ru(OTf)_3$ and bpy ligand.

Table 2 Catalytic oxidation of cyclooctene to 1,2-epoxycyclooctane by ruthenium(II) complexes in the presence of non-redox metal ions as Lewis acids

Additives	Conversion (%)	Yield (%)
—	21.2	6.7
NaOTf[a]	21.9 (20.5)	5.0 (2.2)
$Mg(OTf)_2$	100 (19.3)	77.0 (2.5)
$Ca(OTf)_2$	100 (11.0)	72.6 (4.4)
$Ba(OTf)_2$	55.9 (12.9)	46.9 (1.7)
$Zn(OTf)_2$	100 (11.9)	68.4 (1.1)
$Sc(OTf)_3$	100 (5.0)	72.5 (2.1)
$Al(OTf)_3$	100 (13.1)	89.9 (3.0)
$Y(OTf)_3$	100 (12.5)	73.1 (3.7)

Conditions: acetone/CH_2Cl_2 (4 : 1, v/v) 1 mL, cyclooctene 0.1 M, *cis*-$Ru(bpy)_2Cl_2$ 1 mM, 2,2′-bipyridine 2 mM, Lewis acid 2 mM, $PhI(OAc)_2$ 0.2 M, 308 K, 10 h. The data in parentheses represent control experiments with Lewis acids only. [a] NaOTf 6 mM.

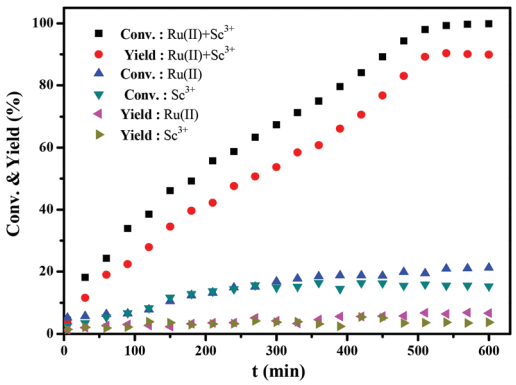

Fig. 1 Kinetics of Lewis acid-accelerated epoxidation by the ruthenium(II) complex. Conditions: solvent: acetone 0.8 mL CH_2Cl_2 0.2 mL, cyclooctene 0.1 M, *cis*-Ru(bpy)$_2$Cl$_2$ 1 mM, 2,2′-bipyridine 2 mM, Al(OTf)$_3$ 2 mM, PhI(OAc)$_2$ 0.2 M, 308 K.

whereas the combination of Ru(II) complex and Lewis acid leads to a remarkable promotion effect. These results are highly consistent with the data in Table 1.

This synergistic oxygen atom transfer by adding non-redox metal ions was also observed in the epoxidation of other *cyclo*-olefins and terminal linear olefins. In all of the investigated substrates, Ru(II) catalyst or Lewis acid alone showed sluggish activity for epoxidation. For example, in Table 3, when cyclohexene was used as the substrate, Ru(II) catalyst alone demonstrated sluggish activity in epoxidation, giving only 15.2% conversion with 3.8% yield of epoxide. Under identical conditions, the addition of 2 equiv. of Al(III) generated high oxidation activity, with 100% conversion and 82.2% yield of epoxide. Similar promotion effects by adding non-redox metal ions can also be observed in the cases of norbornene, styrene and terminal linear olefins such as 1-hexene and 1-dodecene. For example, by adding 2 equiv. of Al(III), the conversion of 1-hexene was increased to 94.6% with 74.6% yield of epoxide, while the conversion of 1-dodecene was increased to 100% with 67.3% yield of epoxide. 36.7% yield of benzaldehyde product was detected by GC when styrene was used as the substrate. To further verify the stability, styrene oxide and 2,3-epoxynorbornane were tested as substrates under identical conditions, while 73.2% 2,3-epoxynorbornane and 82.6% styrene oxide were converted, respectively. Therefore, lower epoxide yield or selectivity for styrene and norbornene were observed in our system. Meanwhile, either Ru(II) catalyst or Lewis acid alone provided limited substance conversion and epoxide yield, which again demonstrates the synergistic effect between Ru(II) catalyst and Lewis acid for the oxygen atom transfer reaction.

Table 3 Al(OTf)$_3$ promoted olefin epoxidations by Ru(bpy)$_2$Cl$_2$ catalyst

Entry	Substrate	Product	Catalyst	Conversion (%)	Yield (%)
1	 cyclooctene	 1,2-epoxycyclooctane	—	12.4	1.4
			Ru(II)	21.2	6.7
			Sc^{3+}	15.2	3.7
			Ru(II) + Sc^{3+}	100	89.9
2[a]	 cyclohexene	 1,2-epoxycyclohexane	—	11.2	3.5
			Ru(II)	15.2	3.8
			Sc^{3+}	5.1	2.8
			Ru(II) + Sc^{3+}	100	82.2
3[b]	 norbornene	 epoxynorbornylene	—	8.4	3.0
			Ru(II)	44.3	15.4
			Sc^{3+}	16.1	3.3
			Ru(II) + Sc^{3+}	98.9	33.6
4[c]	 styrene	 epoxystyrene	—	16.1	0.6
			Ru(II)	21.6	2.4
			Sc^{3+}	15.3	2.7
			Ru(II) + Sc^{3+}	100	30.0
5[d]	 1-hexene	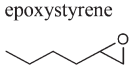 1,2-epoxyhexene	—	5.8	1.6
			Ru(II)	18.8	2.0
			Sc^{3+}	7.5	2.3
			Ru(II) + Sc^{3+}	94.6	74.6
6[d]	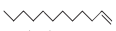 1-dodecene	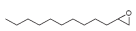 1,2-epoxydodecene	—	5.8	0.9
			Ru(II)	24.1	8.0
			Sc^{3+}	13.4	6.5
			Ru(II) + Sc^{3+}	100	67.3

Conditions: acetone/CH_2Cl_2 (4 : 1, v/v) 1 mL, olefin 0.1 M, *cis*-Ru(bpy)$_2$Cl$_2$ 1 mM, 2,2′-bipyridine 2 mM, Lewis acid 2 mM, PhI(OAc)$_2$ 0.2 M, 308 K, 10 h. [a] 293 K, 6 h. [b] 293 K, 12 h. [c] 293 K, 12 h, 36.7% yield of benzaldehyde was detected by GC. [d] Olefin 0.05 M, Ru(II) complex 0.5 mM, 2,2′-bipyridine 1 mM, Lewis acid 1 mM, PhI(OAc)$_2$ 0.1 M, 308 K, 2 h.

Reaction mechanism

The reaction data presented above clearly reveal that a synergistic effect exists between $Ru(bpy)_2Cl_2$ and non-redox metal ions as Lewis acids in the catalysis of olefin epoxidation, which is the first example where non-redox metal ions as Lewis acids accelerate direct oxygen atom transfer catalyzed by ruthenium catalysts. Based on our previous studies and results from other labs, the promotional effects of those non-redox metal ions were generally attributed to their linkages to the redox metal ions through the M^{n+}=O functional group.[52–57,59,63,64,73] In literature reports, the active site of the Ru center for epoxidation is commonly recognized as Ru(IV)=O,[3,5,32–36,74] which prompted us to explore the origin of the increase in catalytic reactivity as follows.

Epoxidation pathway in the absence of Lewis acid. The electronic absorption data for the complex and the kinetic changes of the spectra during stoichiometric oxidation are illustrated in Fig. 2. Due to the interfering UV absorption from acetone in the mixed solution, only signals beyond 320 nm were shown herein. $Ru(bpy)_2Cl_2$ alone gives two district absorption bands (Fig. 2a), an intense band centered at 380 nm and another broad band from 450 nm to 800 nm with λ_{max} at 560 nm. The lowest energy bands in the visible region for these Ru(II) complexes are generally associated with metal-to-ligand charge transfer (MLCT) states resulting from the promotion of an electron from a metal d-orbital to the π*-orbital of the bpy ligand (d → π*). The electronic transitions centered at 380 nm have previously been assigned to both LMCT (π → e_g*) and MLCT (d → π*).[75] For the Ru–Cl complexes, the MLCT bands are red shifted with regard to the analogous $Ru(bpy)_3^{2+}$ species (λ_{max} at 450 nm) because of the relative stabilization of the dπ(Ru) levels provoked by the chloro ligand.[43,75]

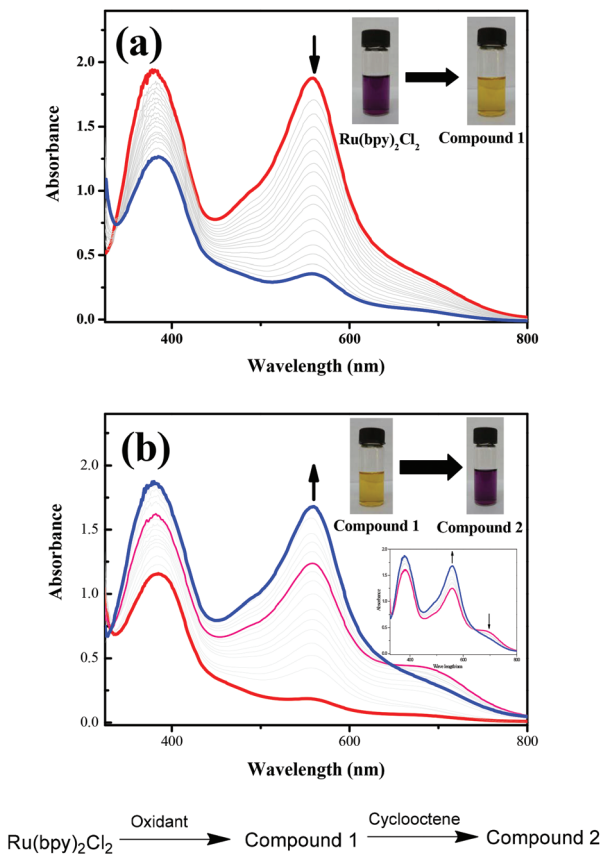

Fig. 2 (a) UV-Vis absorption spectral changes of $Ru(bpy)_2Cl_2$ (0.3 mM) upon addition of 5 equivalents of $PhI(OAc)_2$ at 308 K in acetone/CH_2Cl_2 (1 : 1, v/v). (b) UV-Vis absorption spectral changes of (a) upon addition of 20 equivalents of cyclooctene (red line: initial absorption spectrum, blue line: eventual absorption spectrum, inset: unexpected peak at 680 nm that appears then decays during the process of reduction by cyclooctene).

Upon addition of 5 equiv. of $PhI(OAc)_2$ as oxidant, the deep purple color of $Ru(bpy)_2Cl_2$ gradually changed to yellow, and we named this unknown species compound **1** (Fig. 2(a)). The above oxidation process was much slower compared to the case of adding Lewis acid (*vide infra*, Fig. 5). The concomitant change in the absorption spectra was identical: the molar extinction coefficient of the absorption peak at 380 nm decreased from $\varepsilon = 6.3 \times 10^3$ M^{-1} cm^{-1} to $\varepsilon = 4.2 \times 10^3$ M^{-1} cm^{-1}, whereas the distinct band at 560 nm decreased from $\varepsilon = 6.2 \times 10^3$ M^{-1} cm^{-1} to $\varepsilon = 1.2 \times 103$ M^{-1} cm^{-1}. The absorption spectrum of compound **1** is highly consistent with previous results for the $(bpy)_2Ru(IV)$=O species,[76–79] which gives the first evidence of our proposed reaction pathway: Ru(II) is oxidized to the Ru(IV)=O species using $PhI(OAc)_2$ as a stoichiometric oxidant.[11,25,80] Upon addition of 20 equiv. of cyclooctene as the substrate, this yellow solution of high valent species, $(bpy)_2Ru(IV)$=O, gradually changes back to deep purple. This reduced species is named compound **2**, which showed an identical electronic absorption spectrum to that of $Ru(bpy)_2Cl_2$ (Fig. 2(b)). Moreover, along with the reduction of high valent ruthenium species, the epoxide product can be found by GC-MS analysis. Therefore, the above evidence clearly demonstrates that in the absence of Lewis acid, $(bpy)_2Ru(IV)$=O was generated as the key intermediate and was responsible for the direct oxygen transfer to the substance, after which the Ru(IV)=O species was reduced back to Ru(II) to complete the catalytic cycle. Meanwhile, a weak but nonetheless detectable shoulder peak appeared at around 680 nm and then decayed during the process of oxygen atom transfer from the high valent ruthenium species to cyclooctene (inset in Fig. 2b). This shoulder peak may be attributed to a small amount of Ru(III)–O–Ru(III) dimer originating from the comproportionation of Ru(IV)=O and Ru(II) (*vide infra*). Eventually, this shoulder peak disappeared and an identical absorption spectrum of $Ru(bpy)_2Cl_2$ was regenerated upon addition of extra cyclooctene, implying that the catalytic cycle occurs between the Ru(II) and Ru(IV)=O species.

The above reaction pathway was further confirmed by the change in the NMR spectra (Fig. 3). Initially, the ^1H NMR spectrum of $Ru(bpy)_2Cl_2$ was identical to the reported value of *cis*-$[Ru(bpy)_2–Cl_2]$.[81] Eight resonances appear from 16 protons of the two bipyridyl rings chelated to Ru(II), and the assignments of the above resonances are listed in Fig. S1.† Upon the addition of 5 equiv. of $PhI(OAc)_2$, 16 resonances with the same

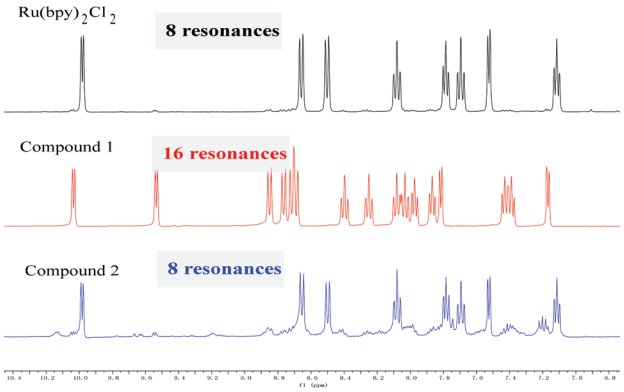

Fig. 3 ^{1}H NMR spectra of ruthenium complexes. Compound **1**: $Ru(bpy)_2Cl_2$ upon addition of 5 equivalents of $PhI(OAc)_2$ (extra PhI and oxidant were removed by washing and recrystallization); compound **2**: compound **1** upon addition of 20 equiv. of cyclooctene.

integral area indicated that 16 protons of the two bipyridyl rings became non-equivalent after the oxidation. This unsymmetrical high valent ruthenium complex (compound **1**) is proposed to have coordination as a Ru(IV)═O species, perhaps *cis*-[Ru(IV)═O$(bpy)_2Cl_2$], which is possible due to the following reasons: (1) EPR studies demonstrate that the high valent ruthenium species exist in the form of Ru(IV) rather than Ru(VI) (see EPR section). (2) A six-coordinate Ru(IV)-oxo complex should be in the S = 1 spin state and thus should be paramagnetic.[82–86] The well-resolved spectra shown in Fig. 3 and 8 disclosed that the Ru(IV) complexes should be seven-coordinate in the S = 0 spin state with a coordination structure as *cis*-[Ru(IV)═O$(bpy)_2Cl_2$].[31,82,84,87,88] (3) The 16 non-equivalent protons of the two bipyridyl rings indicated that the coordination of Ru(IV) species was in the *cis* form. In the case of *trans*-[$(bpy)_2Cl_2$Ru(IV)═O], it will give only 8 non-equivalent protons due to axial symmetry. (4) When we attempted to grow a crystal of the high valent Ru complex that is believed to be responsible for the epoxidation, an unexpected single crystal of Ru(III) complex, *cis*-[$Ru(bpy)_2Cl_2$](OTf), was collected and analyzed (see Fig. S7 and Table S4†). This Ru(III) complex showed no epoxidation reactivity towards the olefin, and was proposed to be generated from the reduction of instable high-valent Ru species. *cis*-[$Ru(bpy)_2Cl_2$](OTf) was found to have two chloro ligands coordinated to the central ion, whereas OTf^- anion acts as a counterion in the outer coordination sphere of Ru(III). From the single crystal structure of this reduced Ru(III) complex, one may conclude that the chloro ligand is more likely to be coordinated to the high-valent Ru(IV) ions than the OTf^- ligand. This single crystal structure also reveals that the promotional effect cannot be attributed to the presence of OTf^- anion.

When extra cyclooctene was added as the substrate to the high valent ruthenium species (compound **1**), the reduced ruthenium species (compound **2**) was obtained and gave an identical ^{1}H NMR spectrum to $Ru(bpy)_2Cl_2$; the epoxide product can be found by GC-MS analysis at the same time. Together with the electronic absorption data mentioned above, compound **2** can be confirmed as $Ru(bpy)_2Cl_2$. Very small peaks from high valent ruthenium species were found in the ^{1}H NMR spectrum of compound **2**, possibly due to the presence of a small amount of $PhI(OAc)_2$ to oxidize the $Ru(bpy)_2Cl_2$ (Fig. 3, compound **2**, blue line). It is thus inferred that the epoxidation pathway in the absence of Lewis acid can be described as follows: Ru(IV)═O (compound **1**), generated from the oxidation of $Ru(bpy)_2Cl_2$, transfers an oxygen atom to the olefin and is reduced back to $Ru(bpy)_2Cl_2$ (compound **2**) to complete the catalytic cycle. The above reaction pathway is clear but not efficient, as evidenced by the epoxidation data in Table 3.

Epoxidation pathway in the presence of Lewis acid. The electronic absorption data for stoichiometric oxidation with the addition of Lewis acid are illustrated in Fig. 4. In the control experiments, neither $Al(OTf)_3$ nor $PhI(OAc)_2$ gave any absorption bands beyond 350 nm. Upon addition of $PhI(OAc)_2$, the MLCT (d → π*) absorption of Ru(II)$(bpy)_2^{2+}$ at 560 nm vanished immediately in the presence of $Al(OTf)_3$, which indicates a much faster oxidation process compared with the case without $Al(OTf)_3$ (Fig. 5). This absorption kinetics is highly consistent with the epoxidation kinetics of the Ru(II) catalyst shown in Fig. 1, indicating that the oxidation from Ru(II) to Ru(IV) was enormously accelerated by Lewis acid. Herein, we named this high valent ruthenium complex compound **3**. Surprisingly, when 20 equiv. of cyclooctene was added as the substrate in the presence of Lewis acid, oxygen atom transfer from compound **3** to the olefin led to another unexpected ruthenium species with a distinct absorption band centered at 650 nm (Fig. 2b), named compound **4**. As shown in Fig. 4c, compound **4** and compound **2** gave distinguished electronic absorption bands, suggesting that an alternative reaction pathway occurs when catalytic epoxidation is conducted in the presence or absence of Lewis acid.

Under the oxidation conditions described above, this ruthenium species can be regenerated for several cycles, which further evidences its role in the catalytic cycle. Initially, compound **3** was prepared by the oxidation of $Ru(bpy)_2Cl_2$. When an excess amount of cyclooctene was added to the solution at T = 0 min (Fig. 5, red line), it initiated a slow growth of the characteristic absorption signal at 650 nm, demonstrating the formation of the reduced ruthenium species, compound **4**. Then, adding $PhI(OAc)_2$ triggered a much faster oxidation from compound **4** to compound **3** to complete the catalytic cycle, and this oxidation process was manifested by the immediate decay of the band at 650 nm. Once again, with the addition of extra cyclooctene, $PhI(OAc)_2$ was consumed while the reduced ruthenium species was regenerated, as observed by the recovery of its absorption at 650 nm. This regeneration can be repeated several times without any loss of the active catalyst (see the intensity of the band at 650 nm after each cycle), which further confirms that this unknown species was involved as the key intermediate in the catalytic cycle in the presence of Lewis acid. As can be seen, the oxidation of compound **3** to compound **4** is significantly faster than the epoxi-

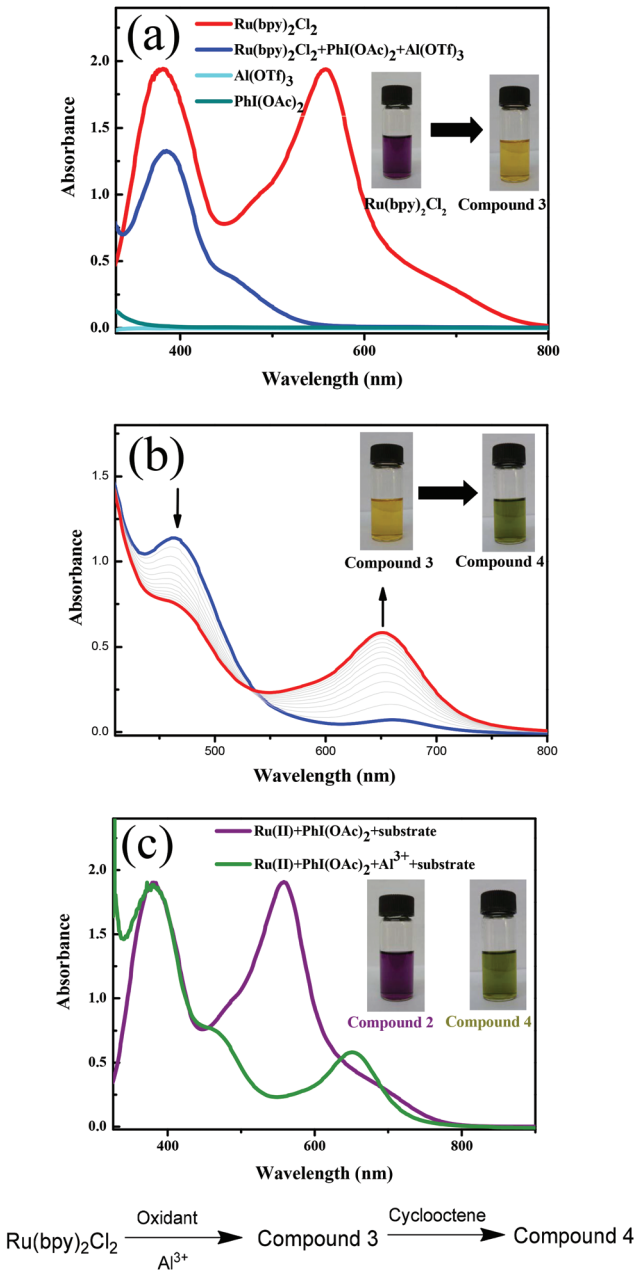

Fig. 4 (a) UV-Vis absorption spectra of compound **3** (0.3 mM $Ru(bpy)_2Cl_2$ upon addition of 5 equivalents of $PhI(OAc)_2$ and 2 equivalents of $Al(OTf)_3$). (b) UV-Vis absorption spectra of compound **4** (0.3 mM compound **3** upon addition of 20 equiv. of cyclooctene.) (c) UV-Vis absorption spectra of compound **2** and compound **4**. Conditions: $Ru(bpy)_2Cl_2$ in acetone/CH_2Cl_2 (1 : 1, v/v) at 308 K.

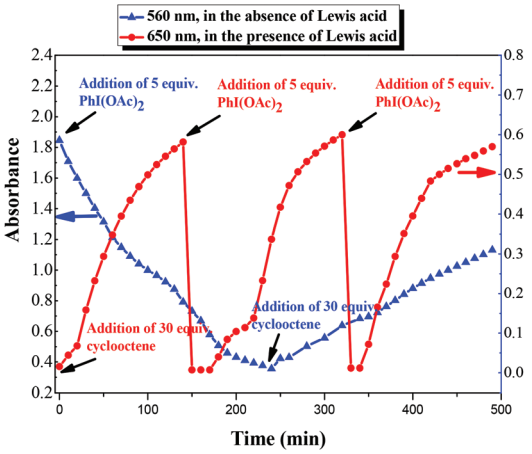

Fig. 5 Kinetic trace at 560 nm corresponding to a reaction mixture of $Ru(bpy)_2Cl_2$ (0.3 mM), 5 equivalents of $PhI(OAc)_2$, and 30 equivalents of cyclooctene at 308 K and a trace at 650 nm corresponding to a reaction mixture containing $Ru(bpy)_2Cl_2$ (0.3 mM), 5 equivalents of $PhI(OAc)_2$, 2 equivalents of $Al(OTf)_3$ and 30 equivalents of cyclooctene at 308 K.

dation step, indicating that the rate-determining step (rds) of this catalysis involves the interaction of the double bond of the alkene with Ru(IV)=O groups and eventual transfer of the oxygen atom to the olefin. Similarly, a kinetic trace at 560 nm corresponding to the reaction in the absence of Lewis acid was also recorded under identical conditions. According to our previous discussion for the case without Lewis acid, the absorption at 560 nm represented the $Ru(II)(bpy)_2^{2+}$ species, and the disappearance of this peak indicated the oxidation from $Ru(II)(bpy)_2^{2+}$ to Ru(IV)=O, followed by reduction back to $Ru(II)(bpy)_2^{2+}$ upon addition of extra cyclooctene. As can be seen, the catalytic reaction rate was obviously accelerated with the addition of Lewis acid, and more importantly, the reaction pathways are totally different in the absence and presence of Lewis acid. Thus, collecting the valence and coordination information of compound **4**, with the absorption peak at 650 nm, is essential to understand the mechanism of Lewis acid-accelerated-epoxidation.

A Ru-bpy based complex that possesses a similar absorption band centered at 672 nm was first prepared and well characterized as an oxo-bridged Ru(III) dimer, $[(bpy)_2ClRu(III)–(\mu\text{-}O)–Ru(III)Cl(bpy)_2]^{2+}$, by Meyer and co-workers.[89] $[(bpy)_2(H_2O)Ru(III)–(\mu\text{-}O)–Ru(III)(H_2O)(bpy)_2]^{4+}$ also showed a very similar absorption peak at 660 nm. DFT calculation indicated that the band around 650 to 670 nm can be assigned mainly to the transition from $d\pi(Ru^{III}–O–Ru^{III})$ to $d\pi^*(Ru^{III}–O–Ru^{III})$; thus, ruthenium dimers with other states show distinguished electronic absorption bands.[90,91] Alternatively, Ru(III)/Ru(IV) dimers such as $[(bpy)_2ClRu(III)–(\mu\text{-}O)–Ru(IV)Cl(bpy)_2]^{2+}$ showed a distinct absorption band centered at 470 nm,[81,89] and no signal could be observed in the region of 600 to 700 nm from either Ru(III)–(μ-O)–Ru(IV) or Ru(IV)–(μ-O)–Ru(IV) with bpy ligand.[92] The above results strongly suggest that our unexpected species, compound **4**, which can be generated from the oxygen transfer reaction between high valent Ru(IV) species and olefin in the presence of Lewis acid, is an oxo-bridged Ru(III) dimer.

To further verify the oxidation states of ruthenium in compound **4**, X-ray photoelectron data of the different ruthenium complexes were collected, and the results are illustrated in Fig. 6. Peaks occurring in the region of 272 to 292 eV were attributed to ruthenium ($Ru\ 3d_{3/2}$ and $Ru\ 3d_{5/2}$) and carbon (C 1s) electron transitions. Herein, all binding energies were

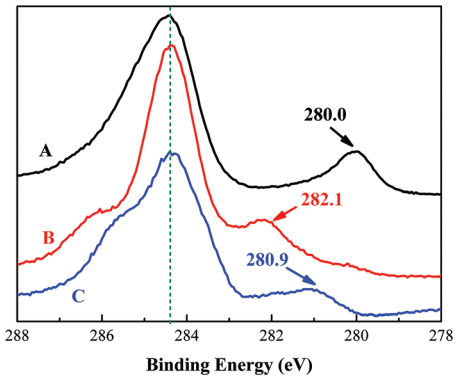

Fig. 6 X-ray photoelectron emission spectra of $Ru(bpy)_2Cl_2$ (A); $[Ru(bpy)_2Cl_2](CF_3SO_3)$ (B); compound **4** (C). The C 1s reference peak is defined as 284.4 eV in all cases.

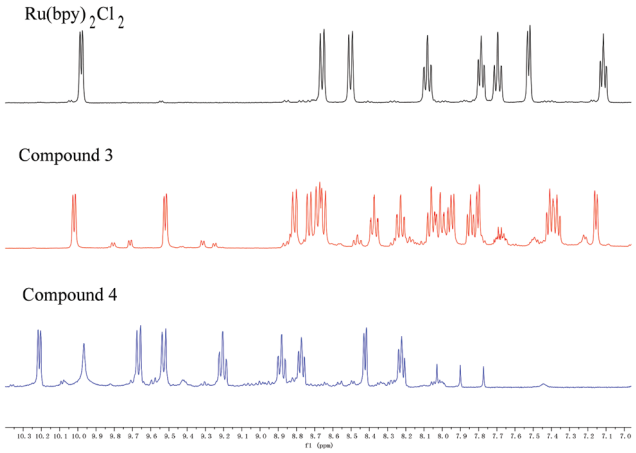

Fig. 7 ^{1}H NMR spectra of the ruthenium complexes. Compound **3**: $Ru(bpy)_2Cl_2$ upon addition of 2 equivalents of $Al(OTf)_3$ and 5 equivalents of $PhI(OAc)_2$ (extra PhI and oxidant were removed by washing and recrystallization); compound **4**: compound **3** upon addition of 20 equivalents of cyclooctene.

measured relative to an arbitrarily assigned value of 284.4 eV, which is due to the C 1s peak from the bpy ligand, because the absolute binding energies varied somewhat from sample to sample due to surface charging effects.[89] *cis*-Ru(II)$(bpy)_2Cl_2$ was first measured as the standard and showed a binding energy of 280.0 eV for the Ru 3d5/2 peak. This result is in excellent agreement with the value obtained in the literature (279.9 eV for *cis*-Ru(II)$(bpy)_2Cl_2$).[89] The single crystal of Ru(III) complex $[Ru(III)(bpy)_2Cl_2](OTf)$ gave a binding energy of 282.1 eV, which is also in good agreement with previously found values for Ru(III) (281.9 eV for $[Ru(III)(bpy)_2Cl_2]Cl$). In the case of compound **4**, a broadening ruthenium peak was detected with a value of 280.9 eV, also consistent with Ru $3d_{5/2}$, that is, Ru(II) < Ru(III)–O–Ru(III) < Ru(III). Our results also follow this rule, which further supports the hypothesis previously supported by the electronic absorption results that compound **4** can be recognized as an oxo-bridged Ru(III). Also, the lack of splitting of the Ru $3d_{3/2}$ and Ru $3d_{5/2}$ peaks for compound **4** indicates that the two ruthenium centers are equivalent, or nearly equivalent.

The above XPS data, together with evidence from the electronic absorption data, suggest that compound **4** is a Ru(III)/Ru(III) dimer with bpy ligand. In recent years, related spectral characterization and redox properties of such ruthenium dimers with bpy analogues as ligands, well-known as the "blue-dimer", have received intense scientific scrutiny because they are recognized as the key precursors to release molecular oxygen in water oxidation.[27,32,93–96] However, oxo-bridged Ru(III) dimers were seldom reported as an intermediate in catalyzed epoxidation, even though some well-designed dinuclear ruthenium complexes containing organic bridging ligands have been prepared as redox catalysts in olefin epoxidation.[3,5,6]

The epoxidation reaction in the presence of Lewis acid was also monitored by NMR spectroscopy, and the results are shown in Fig. 7. Upon addition of 2 equiv. of Lewis acid and 5 equiv. of $PhI(OAc)_2$, 16 resonances with the same integral area were observed for compound **3**, demonstrating that 16 protons of the two bipyridyl rings became non-equivalent after the oxidation. This unsymmetrical high valent ruthenium complex (compound **3**) can be assigned as an adduct of Ru(IV)=O/Al(III) species, possibly *cis*-[Ru(IV)=O$(bpy)_2Cl_2$]/Al(III), based on the following reasons: (1) EPR study demonstrates that the high valent ruthenium species exists in the form of Ru(IV) rather than higher states such as Ru(V) or Ru(VI) (see EPR section). (2) The ^{1}H NMR signal of compound **3** is similar to, but not the same as that of compound **1**, Ru(IV)=O. The differences in the chemical shifts of the protons between compound **3** and compound **1** may be induced by the linkages of the non-redox metal ion to the Ru(IV)=O functional group (*vide infra*). Surprisingly, with the addition of an extra amount of cyclooctene, only 8 resonances appear for compound **4**. As can be seen, the chemical shifts of these 8 resonances are clearly different from those of *cis*-$Ru(bpy)_2Cl_2$, which is consistent with the results of the electronic spectra shown in Fig. 4c and further demonstrates that adding Lewis acid has changed the epoxidation pathway of the ruthenium catalyst. There are two speculations to explain these 8 resonances in compound **4**, which has been previously proposed to be a Ru(III)/Ru(III) dimer. The first speculation arises from the possibility that one bpy ligand is dissociated from the metal ion during the redox process, and only one bipyridine is coordinated to each Ru(III) ion. Therefore, the remaining two bpy ligands are equivalent in chemical environment and thus give 8 resonances from 16 protons. However, the above speculation on the dissociation of the complex is not favored because the consumption and regeneration of compound **4** can be easily repeated without any decrease in the content of active ruthenium species (see Fig. 4). Furthermore, resonances from the protons in dissociated bpy ligand should be observed in the NMR spectra as well as the ligated bpy, which is obviously not the case in Fig. 7. The other explanation is that 8 resonances appear from 4 equivalent bpy ligands due to a higher level symmetry from the geometric point of view; based on this, compound **4** can

be speculated as a di-oxo bridged Ru(III) dimer, $[(bpy)_2Ru(III)–(\mu\text{-}O)_2–Ru(III)(bpy)_2]^{2+}$. On the basis of the well-investigated ^1H NMR information of bpy ligand and *cis*-$Ru(bpy)_2Cl_2$, detailed assignments of resonances originating from compound **4** re listed in Fig. S2 and Table S3.†

Another aspect that is worthy of discussion is how the Lewis acid influences the electronic factor of high valent Ru(IV)═O species, which plays a pivotal role in oxygen atom transfer. As mentioned above, in the absence of Lewis acid, compound **1** was generated from the chemical oxidation of $Ru(bpy)_2Cl_2$ and was recognized as Ru(IV)═O based on various photonic and electronic characterizations. Meanwhile, with the addition of Lewis acid, the generated compound **3** also showed 16 resonances with the same integral area, indicating 16 non-equivalent protons in two bpy ligands. However, the chemical shifts of the protons in compound **3** were different from those of compound **1**. To assign each proton accurately and to further explore the interaction between the Lewis acid and the Ru(IV)═O species, the ^{13}C NMR and $^1H–^{13}C$ HSQC spectra of compound **3** were measured and are shown in Fig. S3.† We initialized the assignment according to the ^{13}C NMR results: the electron density of the carbons in the pyridine ring follows the order of *ortho-* > *para-* > *meta-*, leading to a stronger deshielding effect in the *ortho*-position and showing a chemical shift to a lower field. The above trend is consistent in both the free and coordinated ligands. Thus, assignment of the ^{13}C resonances in compound **3** followed straightforwardly from the ^{13}C NMR spectra of bpy ligand and $Ru(bpy)_2Cl_2$,[81] and these results are shown in Fig. S3.† Together with the $^1H–^{13}C$ HSQC spectrum, the resonances of each proton in compound **3** were carefully assigned and are summarized in Table S3.†

On the basis of the above assignments and analysis, the ^1H NMR spectra of compound **1** and compound **3**, which are respectively recognized as the key intermediates for the oxygen atom transfer in the different reaction pathways, are compared in Fig. 8. Some peaks in the black line in Fig. 8 located at 7.1 to 7.8 ppm are due to unreacted $PhI(OAc)_2$ and PhI. Among all these resonances, those in the region of 8.88 to 8.65 ppm show the most obvious shifts with the addition of Al(III). These resonances are assigned to the four protons at the 4,4′,5,5′ positions, as shown in Fig. S3.† Compared with compound **1**, all the resonances were located at a higher field in compound **3** (8.85 to 8.62 ppm). The protons at the 4′ and 4 positions in compound **1** individually show a doublet structure with J = 9 Hz and overlap each other, appearing as a triplet structure (8.72 to 8.66 ppm). Alternatively, in compound **3**, these two doublet structures with J = 8 Hz (8.70 to 8.63 ppm) become separated and appear as a hyperfine structure of four peaks. The above data clearly demonstrate that the linkage of Al(III) to the Ru(IV)═O center leads to a weaker deshielding effect on the protons in the bpy ligand. We believe that the changes in the chemical shifts can be attributed to a perturbation of the magnetic anisotropy rather than an influence on the electron density through a conjugative or inductive effect, based on the following speculations. Considering electronic factors, the linkage of Al(III) to the Ru(IV)═O center should not greatly influence the electron density of the protons at the 2,7 positions in bipyridine because they are separated by three or more bonds. Alternatively, introducing $Al(OTf)_3$ into the Ru(IV)═O center may significantly disturb the geometric factor in the complex due to the steric hindrance of the triflate moiety; this causes certain changes in the magnetic anisotropy and thus, in turn, influences the chemical shifts of the protons. The protons at the 4,5 positions, the chemical shifts of which are located at a lower field than those of the other protons in the *para*-positions of bipyridine (protons at the 2,7 positions) due to the shielding effect from both pyridine rings, are more sensitive to changes in the geometric environment in the ruthenium complex. Therefore, these protons provide the most obvious changes in the ^1H NMR spectra with the addition of Lewis acid. In particular, compound **1** together with 6 equiv. of NaOTf as additive was also measured and listed for the purpose of comparison. In this case, no concomitant change in the ^1H NMR spectrum can be observed, clearly supporting that the $Al(OTf)_3$-induced shifting in the ^1H NMR spectrum was not due to the presence of OTf^-, which is in good agreement with our catalytic epoxidation data (Table 2).

EPR is uniquely sensitive to paramagnetic intermediates. Mononuclear Ru(II) and Ru(IV) are EPR silent, while the mononuclear Ru(III) center gives characteristic EPR signals.[97] Fig. 9 shows the EPR spectra of $Ru(II)(bpy)_2Cl_2$ that underwent oxidation by $PhI(OAc)_2$. Initially, the signal from the mononuclear Ru(II) center was almost silent. However, some weak but detectable peaks corresponding to Ru(III) can be observed under the experimental conditions. This is due to the fact that $Ru(II)(bpy)_2Cl_2$ was synthesized using $RuCl_3$ as a precursor through reduction, during which a trace amount of Ru(III) residue may still remain in the recrystallized Ru(II) catalyst and may easily be observed due to the EPR silence of the Ru(II) center. Upon addition of excess of $PhI(OAc)_2$ as oxidant and freezing within a certain time after mixing, $Ru(II)(bpy)_2Cl_2$ undergoes oxidation, during which distinct signals with g_{xx} = 2.60, g_{yy} = 2.40 and g_{zz} = 1.66 can be observed, indicating the formation of

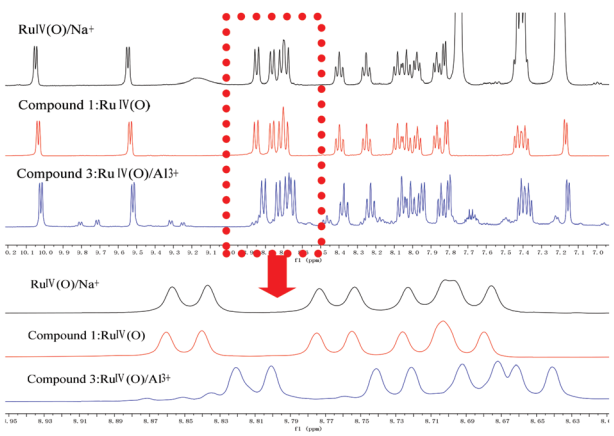

Fig. 8 ^1H NMR spectra of high valent ruthenium complexes with different Lewis acids.

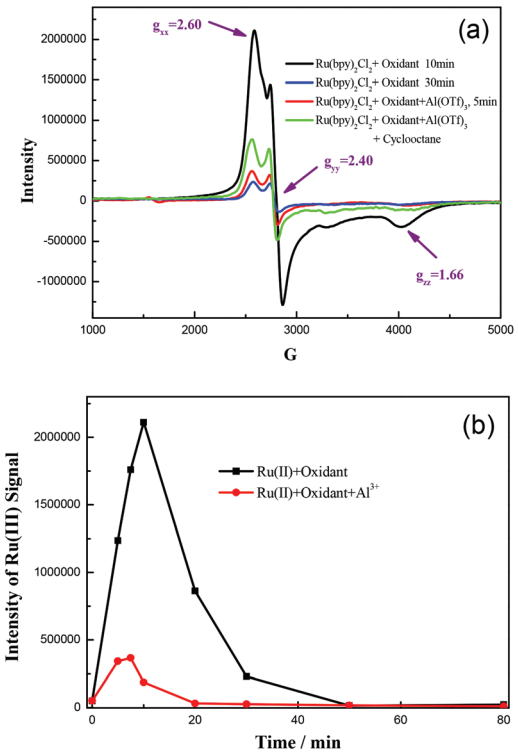

Fig. 9 (a) EPR spectra of the ruthenium complex with oxidant and $Al(OTf)_3$ as additive. (b) Change in the intensity of ruthenium complex at g = 2.60. Conditions: *cis*-$Ru(bpy)_2Cl_2$ 1 mM, 5 equivalents of $PhI(OAc)_2$, 2 equivalents of $Al(OTf)_3$, 20 equiv. of cyclooctene, 130 K.

paramagnetic Ru(III) species. The formation of this Ru(III) species is more likely due to the comproportionation of fresh generated Ru(IV) and the remaining Ru(II) species. Then, the characteristic signal from the Ru(III) species decays along with further oxidation, and the residual EPR signal exhibits an intensity of less than 5% compared with the highest value. The above phenomenon clearly demonstrates the formation and disappearance of the Ru(III) species and furthermore suggests the formation of the Ru(IV)═O moiety in compound **1**. The ruthenium species at higher valences (Ru(V) or Ru(VI)) were not favored in our proposed mechanism because the Ru(V)═O species is more isotropic in comparison with Ru(III) and has very characteristic signals and hyperfine splittings.[98] For instance, the experimental EPR spectra of *cis*-Ru(V)(O)(OH)$(bpy)_2$ showed a distinct signal in the region of 3200 to 3300 G.[99] However, the abovementioned signals from the Ru(V) center were not detected during the oxidation process in this case, which implies that no further oxidation such as Ru(IV) → Ru(V) or Ru(IV) → Ru(VI) is occurring. In the case of oxidation with the addition of Lewis acid, the abovementioned formation and disappearance of the Ru(III) species was much faster, as shown in Fig. 9b, because the oxidation from Ru(II) to Ru(IV)═O was significantly accelerated by the addition of Lewis acid. This phenomenon is also in good agreement with the acceleration demonstrated in the electronic absorption spectra (Fig. 4a and 5). Furthermore, compound **4** exhibits no EPR signal, and this EPR silence is in agreement with the relatively large antiferromagnetic spin–spin coupling of the Ru(III)/Ru(III) dimer.[100]

Generally, epoxidation of *cis*-stilbene can provide further mechanistic information because the ratio of *cis* and *trans*-epoxide products from *cis*-stilbene is highly dependent on the reaction pathway as well as the coordination environments of the redox metal ions. At least two pathways have been reported with distinctly different transition states:[101,102] (1) the radical path, in which direct attack of the substrate by the metal-oxo species generates an olefinic C═C π bond-broken radical, followed by a collapse or rotation–collapse process, thus providing a mixture of *cis* and *trans* epoxides;[103,104] (2) concerted oxygen atom transfer, in which 2 + 2 cycloaddition of the M^{n+}═O moiety to olefin generates a metallaoxetane intermediate, followed by its subsequent breakdown to form an epoxide while retaining the steric structure of the olefin.[105,106] Complementarily, in some Ru(IV)═O based catalytic epoxidation reactions, a radical path has also been suggested that leads to the sterically-retained product.[5] Herein, Ru(II) catalyst alone provided 3.4% *cis*-epoxide and 0.3% *trans*-epoxide when *cis*-stilbene was used as the substrate. Adding Al^{3+} can sharply improve the yields of both *cis*- and *trans*-epoxide. For instance, in the presence of 2 equiv. of Al^{3+}, Ru(II) catalyst gave 39.1% yield of *cis*-epoxide and 7.0% yield of *trans*-epoxide (Table 4). Meanwhile, no *cis*/*trans* isomerization takes place for *cis*-stil-

Table 4 Influence of the $Al(OTf)_3$ concentration on the catalytic oxidation of stilbene by the ruthenium(II) complexes

			Yield (%)		
Substrate	Ru(II) : Al^{3+}	Conversion (%)	*cis*-Epoxide	*trans*-Epoxide	Benzaldehyde
cis-Stilbene	0 : 0	12.4	0.9	0.1	6.4
	1 : 0	15.5	3.4	0.3	5.8
	0 : 2	17.7	0.8	0.5	5.7
	1 : 2	74.7	39.1	7.0	15.6
trans-Stilbene	0 : 0	8.5	0	0.2	4.8
	1 : 0	12.9	0	2.0	8.2
	0 : 2	9.8	0	1.0	5.9
	1 : 2	85.5	0	36.2	17.6

Conditions: acetone/CH_2Cl_2 (4 : 1, v/v) 1 mL, olefin 0.1 M, *cis*-$Ru(bpy)_2Cl_2$ 1 mM, 2,2′-bipyridine 2 mM, $PhI(OAc)_2$ 0.2 M, 298 K, 12 h.

bene, which is proved by the fact that no *trans*-stilbene product was found by GC-MS analysis. The above data point towards a mechanism of concerted oxygen atom transfer from the active species, Ru(IV)=O or Ru(IV)=O/Al(III), to the double bond of olefin. Although the ratios of *cis* and *trans*-epoxide products reported herein are difficult to compare directly with other complexes from the literature because the catalysts and oxidants used are different, the results of catalytic epoxidation in this paper are consistent with a general trend that Ru(IV)=O based species provide a certain steric selectivity.[3,5,43] In the case of *trans*-stilbene, $Ru(bpy)_2Cl_2$ combined with 2 equiv. of Al(III) as catalyst provides 36.2% yield of *trans*-epoxide with 17.6% yield of benzaldehyde, while $Ru(bpy)_2Cl_2$ alone gave only 2.0% yield of *trans*-epoxide with 8.2% yield of benzaldehyde. Notably, there was no *cis*-stilbene epoxide formation from *trans*-stilbene.

Another key piece of evidence that the active Ru(IV)=O species is responsible for the oxygen atom transfer reaction comes from ^{18}O isotope labelling experiments (Fig. 10). A metal oxo species can exchange its oxo functional group with ^{18}O-water to form $M^{n+}=^{18}O$ and subsequently incorporate ^{18}O into olefin, forming ^{18}O-epoxide products.[107] In the epoxidation of *cis*-stilbene catalyzed by Ru(II) complex alone, only 4.6% *cis*-epoxide with a 36.0% abundance of ^{18}O and 12.4% benzaldehyde with a 31.9% abundance of ^{18}O were produced when 0.1 mL $H_2{}^{18}O$ was added to 1.0 mL of reaction solution. In the presence of 2 equiv. of $Al(OTf)_3$, the yield of *cis*-epoxide sharply increased to 28.7% with 35.1% ^{18}O abundance, and the yield of benzaldehyde also increased to 36.4% with 33.3% ^{18}O abundance. The above ^{18}O isotope labelling results further bolster the support for the abovementioned mechanism where Ru(IV)=O is responsible for the oxygen atom transfer reaction.

Taken together, in the absence of Lewis acid, the oxidation of $Ru(bpy)_2Cl_2$ generates the Ru(IV)=O species (compound **1**), which transfers the oxygen atom to olefin and then is reduced back to *cis*-$Ru(bpy)_2Cl_2$ (compound **2**) to complete the catalytic cycle; this is a sluggish process. With the addition of $Al(OTf)_3$ as Lewis acid, the oxidation of $Ru(bpy)_2Cl_2$ generates an adduct of Ru(IV)=O and Al(III), proposed as Ru(IV)=O/Al(III) (compound **3**). This adduct can efficiently transfer the oxygen

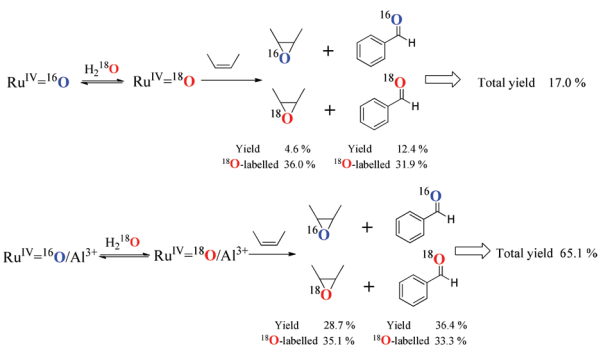

Fig. 10 Isotopic labelling experiments using $H_2{}^{18}O$ for the catalytic oxidation of *cis*-stilbene.

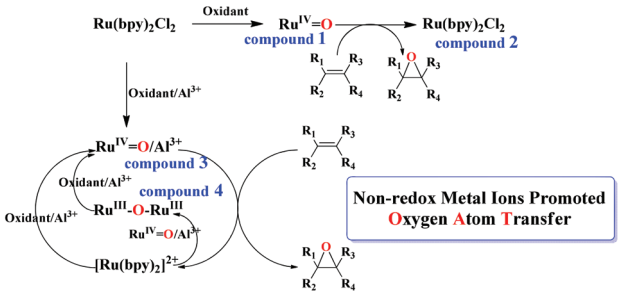

Scheme 2 Reaction pathways of epoxidation.

atom to olefin and leads to the formation of a Ru(III)/Ru(III) dimer (compound **4**) which can be easily oxidized back to compound **3** in the presence of oxidant. As evidenced by the electronic absorption spectra and EPR studies (Fig. 5 and 9b), both the oxygen transfer from Ru(IV)=O/Al(III) to olefin and the oxidation of Ru(III)–O–Ru(III) to Ru(IV)=O/Al(III) are remarkably accelerated by adding Al(III) compared to the case without Al(III). The improved catalytic epoxidation efficiency with the addition of Lewis acid (as shown in Table 1) was also attributed to this acceleration effect (Scheme 2).

To further explore the origin of this Ru(III)–O–Ru(III) dimer, $Ru(II)(bpy)_2Cl_2$ was mixed with one equivalent of high valent Ru(IV)=O/Al(III) (compound **3**), and its UV-Vis spectrum immediately changed to that of compound **4** (as shown in Fig. S9†), supporting the formation of the Ru(III)–O–Ru(III) dimer. This result demonstrated the comproportionation of Ru(IV)=O/Al(III); Ru(II) would generate the Ru(III)–O–Ru(III) species. Theoretically, the oxygen atom transfer from Ru(IV)=O/Al(III) to olefin would generate the Ru(II) species, and the Ru(II) species would be further oxidized to Ru(IV)=O/Al(III) in the presence of Lewis acid to complete the catalytic cycle. However, as demonstrated in Fig. 5, the oxidation of low valent ruthenium complex to Ru(IV)=O/Al(III) is significantly faster than the epoxidation step, indicating that the rate-determining step (rds) of this process involves the interaction of the double bond of the alkene with Ru(IV)=O groups and the eventual transfer of the oxygen atom to the olefin. Thus, Ru(II) species cannot be directly observed in the Lewis acid-accelerated reactions.

Apparently, our results have illustrated a novel strategy to explore the catalytic reactivity of redox metal complexes without chemical modification of their organic ligands under oxidation conditions. To further verify this strategy, ruthenium complexes with different ligands are employed as catalysts for the epoxidation of cyclooctene (Table 5). All these ruthenium complexes alone, as well as $Ru(bpy)_2Cl_2$ catalyst, are very sluggish in olefin epoxidation. For example, $Ru(ptd)_2Cl_2$ (ptd = 1,10-phenanthroline-5,6-dione) alone as the catalyst only gave 28.1% conversion with 10.5% yield in the epoxidation of cyclooctene. Remarkably, the addition of Lewis acid sharply promoted conversion of up to 100% with a 66.4% yield of epoxide. This acceleration has been observed in each case, which further supports the effectiveness of our strategy. That

Table 5 Catalytic oxidation of cyclooctene by Ru(II) complexes bearing various ligands

Ligand	$Al(OTf)_3$ (mM)	Conversion (%)	Yield (%)
bpy[a]	0	21.2	6.7
	2	99.9	89.9
bpm	0	32.2	19.3
	2	100	70.1
dpk	0	63.8	30.8
	2	100	80.2
ptd	0	28.1	10.5
	2	100	66.4
bpp	0	26.2	10.3
	2	80.7	49.6

Conditions: acetone 1 mL, olefin 0.1 M, Ru(II) complex 1 mM, ligand 4 mM, Lewis acid 2 mM, $PhI(OAc)_2$ 0.2 mmol, 298 K, 10 h. [a] Acetone/CH_2Cl_2 (4 : 1, v/v) 1 mL, 2,2′-bipyridine 2 mM, 308 K, 10 h.

is, *in situ* addition of Lewis acid to control the redox behavior through the linkage of the non-redox metal ion to the active M^{n+}=O species results in an improvement in the oxygen atom transfer efficiency. Also, our insights into the catalytic mechanism may shed some light on the geometrical and electronic factors that can favor the oxidation reactivity of ruthenium catalysts.

Conclusions

In this study, we reported the first example in which oxygen atom transfer catalyzed by ruthenium complex with bipyridine ligand was remarkably accelerated by non-redox metal ions, which represents an important enzymatic and chemical oxidative process. Demonstrated by various spectroscopic characterizations, the oxidation of $Ru(bpy)_2Cl_2$ will generate the Ru(IV)=O species (compound **1**), which transfers the oxygen atom to olefin and then is reduced back to *cis*-$Ru(bpy)_2Cl_2$ (compound **2**). This catalytic epoxidation was very sluggish when $Ru(bpy)_2Cl_2$ was tested as the catalyst alone. With the addition of $Al(OTf)_3$ as Lewis acid, the oxidation of $Ru(bpy)_2Cl_2$ generated an adduct proposed as Ru(IV)=O/Al(III) (compound **3**), which is highly active for epoxidation. Alternatively, transferring the oxygen atom onto the olefin leads to a Ru(III)–O–Ru(III) dimer (compound **4**), and this dimer can be easily oxidized back to the high valent species to complete the cycle. The above steps were both accelerated in the presence of Al(III). Our results illustrated a novel strategy to improve the catalytic reactivity of a variety of redox metal complexes. Moreover, the studies demonstrated here may also provide new clues to understand the catalytic mechanism regulated by non-redox metal ions and may also aid the exploration of geometrical and electronic factors that can favor the oxidation reactivity of ruthenium catalysts.

Acknowledgements

This study was supported by the National Natural Science Foundation of China (No. 21303063 and 21273086) and the Graduates' Innovation Fund of Huazhong University of Science and Technology (No. 0118650009). The GC-MS and XPS analysis was performed in the Analytical and Testing Center of Huazhong University of Science and Technology.

Notes and references

1 J. T. Groves and R. Quinn, *J. Am. Chem. Soc.*, 1985, **107**, 5790–5792.
2 L. K. Stultz, R. A. Binstead, M. S. Reynolds and T. J. Meyer, *J. Am. Chem. Soc.*, 1995, **117**, 2520–2532.
3 C. Di Giovanni, L. Vaquer, X. Sala, J. Benet-Buchholz and A. Llobet, *Inorg. Chem.*, 2013, **52**, 4335–4345.
4 Y. Wang, L. Duan, L. Wang, H. Chen, J. Sun, L. Sun and M. S. G. Ahlquist, *ACS Catal.*, 2015, **5**, 3966–3972.
5 J. Aguiló, L. Francàs, R. Bofill, M. Gil-Sepulcre, J. García-Antón, A. Poater, A. Llobet, L. Escriche, F. Meyer and X. Sala, *Inorg. Chem.*, 2015, **54**, 6782–6791.
6 L. Francàs, R. M. González-Gil, D. Moyano, J. Benet-Buchholz, J. García-Antón, L. Escriche, A. Llobet and X. Sala, *Inorg. Chem.*, 2014, **53**, 10394–10402.
7 C. Di Giovanni, A. Poater, J. Benet-Buchholz, L. Cavallo, M. Solà and A. Llobet, *Chem. – Eur. J.*, 2014, **20**, 3898–3902.
8 S. Bhor, M. K. Tse, M. Klawonn, C. Döbler, W. Mägerlein and M. Beller, *Adv. Synth. Catal.*, 2004, **346**, 263–267.
9 S. Funyu, T. Isobe, S. Takagi, D. A. Tryk and H. Inoue, *J. Am. Chem. Soc.*, 2003, **125**, 5734–5740.
10 K. Jitsukawa, Y. Oka, S. Yamaguchi and H. Masuda, *Inorg. Chem.*, 2004, **43**, 8119–8129.
11 M. Dakkach, A. Atlamsani, T. Parella, X. Fontrodona, I. Romero and M. Rodriguez, *Inorg. Chem.*, 2013, **52**, 5077–5087.
12 F. R. Keene, *Coord. Chem. Rev.*, 1999, **187**, 121–149.
13 W. W. Y. Lam, M. F. W. Lee and T. C. Lau, *Inorg. Chem.*, 2006, **45**, 315–321.
14 F. Carson, S. Agrawal, M. Gustafsson, A. Bartoszewicz, F. Moraga, X. D. Zou and B. Martin-Matute, *Chem. – Eur. J.*, 2012, **18**, 15337–15344.
15 G. Csjernyik, A. H. Éll, L. Fadini, B. Pugin and J.-E. Bäckvall, *J. Org. Chem.*, 2002, **67**, 1657–1662.
16 I. W. C. E. Arends, T. Kodama and R. A. Sheldon, in *Ruthenium Catalysts and Fine Chemistry*, ed. C. Bruneau and P. Dixneuf, Springer, Berlin, Heidelberg, 2004, ch. 10, vol. 11, pp. 277–320.
17 J. F. Zhao, C. Muck-Lichtenfeld and A. Studer, *Adv. Synth. Catal.*, 2013, **355**, 1098–1106.
18 B. Liu, F. Hu and B. F. Shi, *ACS Catal.*, 2015, **5**, 1863–1881.
19 D. Srimani, E. Balaraman, B. Gnanaprakasam, Y. Ben-David and D. Milstein, *Adv. Synth. Catal.*, 2012, **354**, 2403–2406.
20 T. Smejkal, H. Han, B. Breit and M. J. Krische, *J. Am. Chem. Soc.*, 2009, **131**, 10366–10367.
21 J. C. Leung, L. M. Geary, T. Y. Chen, J. R. Zbieg and M. J. Krische, *J. Am. Chem. Soc.*, 2012, **134**, 15700–15703.

22 B. Sam, T. Luong and M. J. Krische, *Angew. Chem., Int. Ed.*, 2015, **54**, 5465–5469.
23 M. Z. Wang, C. Y. Zhou, M. K. Wong and C. M. Che, *Chem. – Eur. J.*, 2010, **16**, 5723–5735.
24 M. H. V. Huynh, L. M. Witham, J. M. Lasker, M. Wetzler, B. Mort, D. L. Jameson, P. S. White and K. J. Takeuchi, *J. Am. Chem. Soc.*, 2003, **125**, 308–309.
25 O. Hamelin, S. Menage, F. Charnay, M. Chavarot, J. L. Pierre, J. Pecaut and M. Fontecave, *Inorg. Chem.*, 2008, **47**, 6413–6420.
26 L. Roecker, J. C. Dobson, W. J. Vining and T. J. Meyer, *Inorg. Chem.*, 1987, **26**, 779–781.
27 S. W. Gersten, G. J. Samuels and T. J. Meyer, *J. Am. Chem. Soc.*, 1982, **104**, 4029–4030.
28 C. Sens, I. Romero, M. Rodríguez, A. Llobet, T. Parella and J. Benet-Buchholz, *J. Am. Chem. Soc.*, 2004, **126**, 7798–7799.
29 R. Zong and R. P. Thummel, *J. Am. Chem. Soc.*, 2005, **127**, 12802–12803.
30 L. L. Duan, F. Bozoglian, S. Mandal, B. Stewart, T. Privalov, A. Llobet and L. C. Sun, *Nat. Chem.*, 2012, **4**, 418–423.
31 H.-W. Tseng, R. Zong, J. T. Muckerman and R. Thummel, *Inorg. Chem.*, 2008, **47**, 11763–11773.
32 Y. Tamaki, A. K. Vannucci, C. J. Dares, R. A. Binstead and T. J. Meyer, *J. Am. Chem. Soc.*, 2014, **136**, 6854–6857.
33 C. M. Che, W. Y. Yu, P. M. Chan, W. C. Cheng, S. M. Peng, K. C. Lau and W. K. Li, *J. Am. Chem. Soc.*, 2000, **122**, 11380–11392.
34 H. Tanaka, H. Nishikawa, T. Uchida and T. Katsuki, *J. Am. Chem. Soc.*, 2010, **132**, 12034–12041.
35 W. P. Yip, W. Y. Yu, N. Y. Zhu and C. M. Che, *J. Am. Chem. Soc.*, 2005, **127**, 14239–14249.
36 A. Dovletoglou, S. A. Adeyemi, M. H. Lynn, D. J. Hodgson and T. J. Meyer, *J. Am. Chem. Soc.*, 1990, **112**, 8989–8990.
37 J. C. Dobson, W. K. Seok and T. J. Meyer, *Inorg. Chem.*, 1986, **25**, 1513–1514.
38 R. Neumann and M. Dahan, *Nature*, 1997, **388**, 353–355.
39 E. McNeill and J. Du Bois, *Chem. Sci.*, 2012, **3**, 1810–1813.
40 P. Fackler, S. M. Huber and T. Bach, *J. Am. Chem. Soc.*, 2012, **134**, 12869–12878.
41 M. K. Tse, H. Jiao, G. Anilkumar, B. Bitterlich, F. G. Gelalcha and M. Beller, *J. Organomet. Chem.*, 2006, **691**, 4419–4433.
42 J. Mola, M. Rodriguez, I. Romero, A. Llobet, T. Parella, A. Poater, M. Duran, M. Sola and J. Benet-Buchholz, *Inorg. Chem.*, 2006, **45**, 10520–10529.
43 I. Serrano, M. I. Lopez, I. Ferrer, A. Poater, T. Parella, X. Fontrodona, M. Sola, A. Llobet, M. Rodriguez and I. Romero, *Inorg. Chem.*, 2011, **50**, 6044–6054.
44 A. K. Pal and G. S. Hanan, *Chem. Soc. Rev.*, 2014, **43**, 6184–6197.
45 S. V. Seetharaman, D. D. Winkler, A. B. Taylor, X. H. Cao, L. J. Whitson, P. A. Doucette, J. S. Valentine, V. Schirf, B. Demeler, M. C. Carroll, V. C. Culotta and P. J. Hart, *Biochemistry*, 2010, **49**, 5714–5725.
46 J. S. Valentine, P. A. Doucette and S. Zittin Potter, *Annu. Rev. Biochem.*, 2005, **74**, 563–593.
47 W. Nam and J. S. Valentine, *J. Am. Chem. Soc.*, 1990, **112**, 4977–4979.
48 Y. H. Yang, F. Diederich and J. S. Valentine, *J. Am. Chem. Soc.*, 1991, **113**, 7195–7205.
49 I. Rivalta, G. W. Brudvig and V. S. Batista, *Curr. Opin. Chem. Biol.*, 2012, **16**, 11–18.
50 R. K. Grasselli, *Top. Catal.*, 2002, **21**, 79–88.
51 Y. H. Yang, F. Diederich and J. S. Valentine, *J. Am. Chem. Soc.*, 1990, **112**, 7826–7828.
52 C. G. Miller, S. W. Gordon-Wylie, C. P. Horwitz, S. A. Strazisar, D. K. Peraino, G. R. Clark, S. T. Weintraub and T. J. Collins, *J. Am. Chem. Soc.*, 1998, **120**, 11540–11541.
53 Z. Zhang, K. L. Coats, Z. Chen, T. J. Hubin and G. Yin, *Inorg. Chem.*, 2014, **53**, 11937–11947.
54 Z. Q. Chen, L. Yang, C. Choe, Z. Lv and G. C. Yin, *Chem. Commun.*, 2014, **51**, 1874–1877.
55 P. Leeladee, R. A. Baglia, K. A. Prokop, R. Latifi, S. P. de Visser and D. P. Goldberg, *J. Am. Chem. Soc.*, 2012, **134**, 10397–10400.
56 Y. J. Park, J. W. Ziller and A. S. Borovik, *J. Am. Chem. Soc.*, 2011, **133**, 9258–9261.
57 J. Park, Y. Morimoto, Y. M. Lee, Y. You, W. Nam and S. Fukuzumi, *Inorg. Chem.*, 2011, **50**, 11612–11622.
58 J. Park, Y. Morimoto, Y. M. Lee, W. Nam and S. Fukuzumi, *J. Am. Chem. Soc.*, 2011, **133**, 5236–5239.
59 Y. Morimoto, H. Kotani, J. Park, Y.-M. Lee, W. Nam and S. Fukuzumi, *J. Am. Chem. Soc.*, 2010, **133**, 403–405.
60 S. Fukuzumi, Y. Morimoto, H. Kotani, P. Naumov, Y.-M. Lee and W. Nam, *Nat. Chem.*, 2010, **2**, 756–759.
61 W. Nam, Y.-M. Lee and S. Fukuzumi, *Acc. Chem. Res.*, 2014, **47**, 1146–1154.
62 F. F. Pfaff, S. Kundu, M. Risch, S. Pandian, F. Heims, I. Pryjomska-Ray, P. Haack, R. Metzinger, E. Bill, H. Dau, P. Comba and K. Ray, *Angew. Chem., Int. Ed.*, 2011, **50**, 1711–1715.
63 D. C. Lacy, Y. J. Park, J. W. Ziller, J. Yano and A. S. Borovik, *J. Am. Chem. Soc.*, 2012, **134**, 17526–17535.
64 S.-M. Yiu, W.-L. Man and T.-C. Lau, *J. Am. Chem. Soc.*, 2008, **130**, 10821–10827.
65 J. P. T. Zaragoza, R. A. Baglia, M. A. Siegler and D. P. Goldberg, *J. Am. Chem. Soc.*, 2015, **137**, 6531–6540.
66 R. A. Baglia, M. Durr, I. Ivanovic-Burmazovic and D. P. Goldberg, *Inorg. Chem.*, 2014, **53**, 5893–5895.
67 M. K. Brennaman, J. H. Alstrum-Acevedo, C. N. Fleming, P. Jang, T. J. Meyer and J. M. Papanikolas, *J. Am. Chem. Soc.*, 2002, **124**, 15094–15098.
68 D. Hong, Y. Yamada, T. Nagatomi, Y. Takai and S. Fukuzumi, *J. Am. Chem. Soc.*, 2012, **134**, 19572–19575.
69 J. Rodríguez-López, M. Shen, A. B. Nepomnyashchii and A. J. Bard, *J. Am. Chem. Soc.*, 2012, **134**, 9240–9250.
70 R. Seidel, M. Faubel, B. Winter and J. Blumberger, *J. Am. Chem. Soc.*, 2009, **131**, 16127–16137.

71 B. P. Sullivan, D. J. Salmon and T. J. Meyer, *Inorg. Chem.*, 1978, **17**, 3334–3341.
72 C. Choe, L. Yang, Z. Lv, W. Mo, Z. Chen, G. Li and G. Yin, *Dalton Trans.*, 2015, **44**, 9182–9192.
73 H. Yoon, Y.-M. Lee, X. Wu, K.-B. Cho, R. Sarangi, W. Nam and S. Fukuzumi, *J. Am. Chem. Soc.*, 2013, **135**, 9186–9194.
74 S. N. Dhuri, K.-B. Cho, Y.-M. Lee, S. Y. Shin, J. H. Kim, D. Mandal, S. Shaik and W. Nam, *J. Am. Chem. Soc.*, 2015, **137**, 8623–8632.
75 P. Pearson, A. M. Bond, G. B. Deacon, C. Forsyth and L. Spiccia, *Inorg. Chim. Acta*, 2008, **361**, 601–612.
76 W. K. Seok and T. J. Meyer, *J. Am. Chem. Soc.*, 1988, **110**, 7358–7367.
77 D. J. Wasylenko, C. Ganesamoorthy, M. A. Henderson, B. D. Koivisto, H. D. Osthoff and C. P. Berlinguette, *J. Am. Chem. Soc.*, 2010, **132**, 16094–16106.
78 B. A. Moyer and T. J. Meyer, *Inorg. Chem.*, 1981, **20**, 436–444.
79 A. S. Goldstein and R. S. Drago, *J. Chem. Soc., Chem. Commun.*, 1991, 21–22.
80 M. Dakkach, X. Fontrodona, T. Parella, A. Atlamsani, I. Romero and M. Rodriguez, *Adv. Synth. Catal.*, 2011, **353**, 231–238.
81 A. Baron, C. Herrero, A. Quaranta, M. F. Charlot, W. Leibl, B. Vauzeilles and A. Aukauloo, *Chem. Commun.*, 2011, **47**, 11011–11013.
82 S. Ohzu, T. Ishizuka, Y. Hirai, H. Jiang, M. Sakaguchi, T. Ogura, S. Fukuzumi and T. Kojima, *Chem. Sci.*, 2012, **3**, 3421–3431.
83 T. J. Groves and K. H. Ahn, *Inorg. Chem.*, 1987, **26**, 3831–3833.
84 T. Kojima, Y. Hirai, K. Yoshizawa and S. Fukuzumi, *Angew. Chem., Int. Ed.*, 2010, **49**, 8449–8453.
85 W. H. Lwung, C. M. Che, C. H. Yeung and C. K. Poon, *Polyhedron*, 1993, **12**, 2331–2334.
86 J. C. Dobson, J. H. Helms, W. E. Hatfield and T. J. Meyer, *Inorg. Chem.*, 1989, **28**, 2200–2204.
87 J. J. Concepcion, J. W. Jurss, J. L. Templeton and T. J. Meyer, *J. Am. Chem. Soc.*, 2008, **130**, 16462–16463.
88 L. L. Duan, A. Fischer, Y. H. Xu and L. C. Sun, *J. Am. Chem. Soc.*, 2009, **131**, 10397–10399.
89 T. R. Weaver, T. J. Meyer, S. A. Adeyemi, G. M. Brown, R. P. Eckberg, W. E. Hatfield, E. C. Johnson, R. W. Murray and D. Untereker, *J. Am. Chem. Soc.*, 1975, **97**, 3039–3048.
90 M. Yoshida, M. Kondo, T. Nakamura, K. Sakai and S. Masaoka, *Angew. Chem., Int. Ed.*, 2014, **53**, 11519–11523.
91 I. Lopez, M. Z. Ertem, C. J. Cramer, V. S. Batista and A. Llobet, *Angew. Chem., Int. Ed.*, 2014, **126**, 209–213.
92 J. A. Stull, R. D. Britt, J. L. McHale, F. J. Knorr, S. V. Lymar and J. K. Hurst, *J. Am. Chem. Soc.*, 2012, **134**, 19973–19976.
93 Y. B. Lei and J. K. Hurst, *Inorg. Chem.*, 1994, **33**, 4460–4467.
94 D. Moonshiram, J. W. Jurss, J. J. Concepcion, T. Zakharova, I. Alperovich, T. J. Meyer and Y. Pushkar, *J. Am. Chem. Soc.*, 2012, **134**, 4625–4636.
95 X. F. Yang and M.-H. Baik, *J. Am. Chem. Soc.*, 2006, **128**, 7476–7485.
96 F. Liu, J. J. Concepcion, J. W. Jurss, T. Cardolaccia, J. L. Templeton and T. J. Meyer, *Inorg. Chem.*, 2008, **47**, 1727–1752.
97 Y. Pushkar, D. Moonshiram, V. Purohit, L. F. Yan and I. Alperovich, *J. Am. Chem. Soc.*, 2014, **136**, 11938–11945.
98 A. C. Dengel and W. P. Griffith, *Inorg. Chem.*, 1991, **30**, 869–871.
99 N. Planas, L. Vigara, C. Cady, P. Miro, P. Huang, L. Hammarstrom, S. Styring, N. Leidel, H. Dau, M. Haumann, L. Gagliardi, C. J. Cramer and A. Llobet, *Inorg. Chem.*, 2011, **50**, 11134–11142.
100 S. Ghumaan, B. Sarkar, S. Patra, K. Parimal, J. van Slageren, J. Fiedler, W. Kaim and G. K. Lahiri, *Dalton Trans.*, 2005, 706–712, DOI: 10.1039/b417530a.
101 R. D. Arasasingham, G. X. He and T. C. Bruice, *J. Am. Chem. Soc.*, 1993, **115**, 7985–7991.
102 N. S. Finney, P. J. Pospisil, S. Chang, M. Palucki, R. G. Konsler, K. B. Hansen and E. N. Jacobsen, *Angew. Chem., Int. Ed.*, 1997, **36**, 1720–1723.
103 W. Adam, K. J. Roschmann, C. R. Saha-Möller and D. Seebach, *J. Am. Chem. Soc.*, 2002, **124**, 5068–5073.
104 M. Palucki, N. S. Finney, P. J. Pospisil, M. L. Guler, T. Ishida and E. N. Jacobsen, *J. Am. Chem. Soc.*, 1998, **120**, 948–954.
105 J. P. Collman, J. I. Brauman, B. Meunier, T. Hayashi, T. Kodadek and S. A. Raybuck, *J. Am. Chem. Soc.*, 1985, **107**, 2000–2005.
106 E. M. McGarrigle and D. G. Gilheany, *Chem. Rev.*, 2005, **105**, 1563–1602.
107 J. T. Groves, J. B. Lee and S. S. Marla, *J. Am. Chem. Soc.*, 1997, **119**, 6269–6273.